iJRASET
International Journal For Research in Applied Science and Engineering Technology

INTERNATIONAL JOURNAL FOR RESEARCH

IN APPLIED SCIENCE & ENGINEERING TECHNOLOGY

Volume: 6 **Issue:** VI **Month of publication:** June 2018

DOI: http://doi.org/10.22214/ijraset.2018.6130

www.ijraset.com

Call: 08813907089 | E-mail ID: ijraset@gmail.com

International Journal for Research in Applied Science & Engineering Technology (IJRASET)
ISSN: 2321-9653; IC Value: 45.98; SJ Impact Factor: 6.887
Volume 6 Issue VI, June 2018- Available at www.ijraset.com

Numerical Analysis of Double Pipe Heat Exchanger with and without Strip

Ala Venkata Rao[1], Srivalli Gollamudi[2]
[1]*M Tech Student Department of Mechanical Engineering, VRSEC, Vijayawada.*
[2]*Assistant Professor Department of Mechanical Engineering, VRSEC, Vijayawada.*

***Abstract**: In this communication, the computational fluid dynamics (CFD) technique is used to study the influence of longitudinal strip (circular & square) on the Nusselt number, pressure drop and overall heat transfer coefficient in double pipe heat-exchangers. For this purpose, longitudinal circular and square strips are inserted inside heat-exchangers where various sizes of meshed grill are developed and simulated at various Reynolds numbers by using the CFD soft-ware of Fluent. The validated model, made clear about the objective and the conditions which could exactly facilitate heat transfer throughout double pipe heat exchangers. Following the numerical simulation, proper pressure effect and heat transfer coefficient correlations for various sizes of longitudinal circular and square strip are considered with different flow rates under the turbulent flow. The outcome of this work indicates that longitudinal circular strip could improve the overall heat transfer coefficient when compared to the square strip and the pressure drop in the square strip side is high when compared to the circular strip side.*
Key words**: CFD, Double pipe heat exchanger, Heat transfer coefficient.

I. INTRODUCTION

Double pipe heat exchangers are commonly used heat transfer equipment in commercial and industrial applications due to their small size, ease of manufacturing and compactness. The most common single phase heat transfer fluids are water (W), ethylene glycol (EG), propylene glycol (PG), and engine oil (EO), among others. The heat transfer of these single phase fluids are limited because of their low thermal conductivity values. Ravi Kumar [01] and his team conducted heat transfer experiments for Fe3O4/water Nano fluids in a double pipe U-bend heat exchanger with and without wire coil inserts at different Reynolds numbers (16,000–30,000), different particle concentrations (0.005– 0.06%) and different wire coil inserts of coil pitch to tube inside diameter (p/d) ratios (1, 1.34 and 1.79) The experimental results indicate that, The Nusselt number i for 0.06% volume concentration of Nano fluid is 14.7% and it further increases to 32.03% for the same 0.06% Nano fluid with wire coil inserts of p/d = 1. Syam Sundar et al. [02] obtained results indicate that Nusselt number enhancement, compared to the water data, for the 0.06% volume concentration of the nano fluid is 14.7% and it further increases to 41.29% for the same 0.06% concentration with the longitudinal strip insert with AR equal to 1. Manoj K. Singh et al. [03] observed the use of Fe3O4 nanoparticles in the base fluid gives higher heat transfer coefficient, effectiveness and NTU. The NTU is enhanced by 1.037-times and the effectiveness by 1.024-times for 0.06% nano fluid at Reynolds number of 28,970. Friction factor of 1.092-times was observed 0.06% particle loading at a Reynolds number of 28,970 compared to water. Hiroyuki Shiraiwa [04] and his team modify the heat exchanger design, add the various shafts and pitches with screw blade were inserted in a single heat exchanger tube. in this study as diameter of screw shaft increased and pitch of screw blade was smaller the exchanged heat increased. Rafal Andrzejczyk et al. [05] the baffles are placed in side of the tube due to this baffles increase turbulence.in this study an average Nusselt numbers are up to 50% higher than values for reference type. Yonggang Leia et al. [06] The Numerical analysis had carried out to investigate the thermo-hydraulic performance of the two reformed shell-and-tube heat exchangers with louver baffles. This louver baffles that decrease and eliminate the dead spaces and avoided that decrease the pressure drop in the shell side The numerical results indicated that the heat transfer coefficient per pressure drop of both the shell-and-tube heat exchangers with louver baffles are higher than that of the shell-and-tube heat exchanger with segmental baffles. Piotr Wais [07] and his team introduced the fins were placed in double heat exchanger to increase the heat transfer rate between the heat exchanger surface and the surroundings. Considering the different fin thickness, the obtained results were the heat transfer decreases with the fin thickness increased. Daniele Fiaschi et al. [08] The limited heat transfer coefficient of the internal gas side in the original configuration was improved with a ‘‘twin barrel” solution, with water in the outer annulus and exhaust gas in the inner duct equipped with internal longitudinal fins. The obtained results were the adoption of three staggered and segmented fins led to an increase of 97% with respect to the bare pipe. Gholamreza Bamorovat Abadi [09] and his team the metal-foam-filled tubes enhance the heat transfer mechanism by providing a high surface-area-to-volume ratio. Tthe pressure drop in metal-foam-filled tubes would

obviously be greater than that in empty tubes and the size of metal foam were reduced then the heat transfer coefficient increased. Kashif Nawaz et al. [10] A high porosity metal foam filled with in the double pipe heat exchanger. The obtained results were metal foams with a smaller pore size (40 PPI) have a larger heat transfer coefficient compared to foams with a larger pore size (5 PPI). However, foams with larger pores result in relatively smaller pressure gradients Metal foams with a smaller pore size (40 PPI) have a larger heat transfer coefficient compared to foams with a larger pore size (5 PPI). Javier Bonilla [11] and his team studied a shell and tube heat exchanger model with different (DYCM, QSS, DY and DYTC) degrees of complexity. In solar power plant the working fluid is thermal oil and storage fluid is thermal oil. The obtained results were the DYCM model provides slightly better results with respect to others. QIAN Jin et al. [12] investigated experimentally on a heat exchanger filled with molten salt, this molten salt heat exchangers are key components in some advanced power systems. Heat transfer characteristics of molten salt in the tube side are discussed and compared with three empirical correlations. It had founded that Wu's Equation has better agreement with the experimental data than Gnielinski's and Hausen's Equations in transitional flow region. Bao-Cun Du [13] and his team experimentally studied on the molten salt filled with in the inside tube of double pipe heat exchanger. The obtained results are the segmental baffles on the molten salt heat transfer enhancement in lower flow rate region are better than those in higher flow rate region, and the maximum increment of Nusselt number is 26%. Mehmet Tana et al. [14] experimentally studied the Silica sand as solid particles (2–4 mm), marble (2–5) and quartz (1.2–2.5 mm) sized materials were filled in heat exchanger, so that surface fouling and scaling shaped as intense corrosion and buffer brush over the plate type heat exchanger were minimized and improved the heat enhancement. TingWang [15] and his team studied a meso-channel parallel flow heat exchanger, developed Thus correlations of heat transfer coefficient N_{uf} and friction factor f_f compared with some existing correlations.

II. EXPERIMENT

A. *Experimental Setup*

The schematic diagram of the experimental setup is depicted in Fig.1 two concentric tube heat exchangers, cooling water tank and heating water tank, set of thermocouples, flow meters (both hot and cold), parallel flow and counter flow valves. The test section is a concentric double pipe with a brass inner tube of inner diameter (ID) 0.0167 m and outer diameter (OD) 0.0215 m, and a galvanized iron annulus of inner diameter (ID) 0.0355 m and outer diameter (OD) 0.0426 m, length of the heat exchanger is 1.7 m. The test section has a single-pass. The heat loss from the test section is minimized by wrapping the annulus tube with asbestos rope material. The four thermocouples were installed to measure the inlet and outlet temperatures of the hot fluid and cold fluid. Before using Two flow meters were used to measure the flow rates of cold fluid and hot fluid. The hot fluid was supplied through the inner tube, while the cold fluid, which is the cooling medium, flows through the annulus tube. In the test section, the inner tube and annulus flows have a counter-flow arrangement. The temperature of the cold water (annulus side) was maintained around 30 °C and kept constant flow rate of 0.6 kg/s. The hot fluid (tube side) with constant inlet temperature of 40 °C from the hot fluid tank was supplied through the inner tube at different mass

Fig.1. An experimental setup of double pipe heat exchanger

flow rates from 0.1 kg/sec to 0.6 kg/s. The experiments were conducted sequentially at different mass flow rates 0.1, 0.2, 0.3, 0.4, 0.5, 0.6 kg/sec. Each flow rate is fresh and used in the experiments. The temperatures of cold and hot fluids were recorded at steady state.

TABLE1. Properties of cold fluid

Properties name	Density kg/m3	Thermal conductivity W/m. K	Viscosity Pa.s	Prantal number	Specific heat Kj/kg. K
Valve	997.5	0.6159	0.00079401	5.41	4.178

The pressure drop across the inner tube of the test section was measured by placing a U-tube manometer between both ends of the tube. To achieve this purpose, 4-mm holes drilled at both ends of the inner tube are connected using flexible tubing to the U-tube manometer; mercury (Hg) is the monomeric fluid and the equivalent height is recorded as a function of the mass flow rate. The system reaches steady state after approximately 2 h of operation; under steady state conditions, the readings of four thermocouples are recorded and used for heat transfer calculations. The logarithmic mean temperature difference method is used to calculate the inside heat transfer coefficient of the hot fluid. The heat transfer and friction factor experiments were repeated and the average values (temperatures of thermocouples) were used for Nusselt number and friction factor calculations.

TABLE.2. Properties of hot fluid

Properties name	Density kg/m3	Thermal conductivity W/m. K	Viscosity Pa.s	Prantal number	Specific heat kj/kg. K
Valve	995	0.6280	0.000653715	4.34	4.178

B. Different shapes (circular and square) of strip inserts

The different sizes and shapes (square and circular) (0.001, 0.002, 0.003, 0.004 m) of the aluminium strip inserts used in this study are shown in Fig. 2 The mass flow rate of hot fluid in the inner tube with the strip inserts. The above procedure is repeated and measured the required properties for the calculation of nusselt number and friction factor, is calculated based on the hydraulic diameter. The hydraulic diameter (d_h) is defined as follows:

$$dh = \frac{4A}{P} \qquad (1)$$

Where p is the perimeter, an A the cross-sectional area. The heat conducted by the strip inserts is neglected in the heat transfer calculations.

Calculated parameters

1) Nusselt Number: Rate of heat flow tube-side fluid;

$$Q_h = \dot{m}_h C_h (T_{h,i} - T_{h,o}) \qquad (2)$$

Rate of heat flow annulus-side fluid;

$$Q_c = \dot{m}_c C_c (T_{c,o} - T_{c,i}) \qquad (3)$$

Overall heat transfer coefficient tube-side;

$$U_i = \frac{Q_{avg}}{A_i \left(\frac{\Delta T_1 - \Delta T_2}{\ln\left(\frac{\Delta T_1}{\Delta T_2}\right)} \right)} \qquad (4)$$

Where $Q_{avg} = \frac{Q_h + Q_c}{2}$; $\Delta T_1 = T_{h,i} - T_{c,o}$; $\Delta T_2 = T_{h,o} - T_{c,i}$

For double pipe heat exchangers by neglecting fouling, the relation for overall heat transfer coefficient (tube-side) is given as:

$$\frac{1}{U_i A_i} = \frac{1}{h_o A_o} + \frac{\ln\left(\frac{D_o}{D_i}\right)}{2\pi KL} + \frac{1}{h_i A_i} \qquad (5)$$

Nusselt number

$$Nu_o = \frac{\left(\frac{f}{2}\right)(Re - 1000)pr}{1.07 + 12.7\left(\frac{f}{2}\right)^{0.5}\left(pr^{2/3} - 1\right)} \qquad (6)$$

$$f = (1.58\ln(Re) - 3.82)^{-2} \; ; 2300 < Re < 10^6; \qquad (7)$$

$$0.5 < pr < 2000$$

$$D_h = \frac{4A}{P} = D_o - D_i \qquad (8)$$

where A is the flow area and determined as $A = \frac{\pi}{4}(D_o^2 - D_i^2)$ (9)

The Nusselt number value obtained from Eq. (6) is used to calculate the annulus heat transfer coefficient (h_o) using the hydraulic diameter (D_h) and thermal conductivity of annulus fluid at mean temperature and the equation is given

$$h_o = \frac{Nu_o \times K_o}{D_h} \qquad (10)$$

$$h_i = \frac{Nu_i \times K_i}{D_i} \qquad (11)$$

This h_i, h_o substitute in the Eq. (5) to obtain the inner tube side heat transfer coefficient

The Reynolds number is based on the flow rate at the inlet of the tube.

$$Re = \left(\frac{\rho v d_i}{\mu}\right) \qquad (12)$$

Friction factor; The friction factor is calculated by the following expression,

$$f = \frac{\Delta P}{\frac{L}{D_i} \times \left(\frac{\rho v^2}{2}\right)} \qquad (13)$$

2) System Modeling through Computational Fluid Dynamics: Computational Fluid Dynamics (CFD) is a technique based on numerical methods which aims at analyzing fluids movement, heat transfer, mass transfer, and chemical reaction. The present study seeks to examine the fluid flow and heat transfer within a heat-exchanger filled with the coiled wire inserts. Therefore, the governing equations including the mass conservation (continuity), momentum conservation, and energy conservation equations are as the following:

Continuity equation;

$$\frac{\partial u_i}{\partial x_i} = 0$$

Momentum equation:

$$\frac{\partial u_i u_j}{\partial x_i} = -\frac{1}{\rho}\frac{\partial p}{\partial x_i} + \frac{\partial}{\partial x_j}\left((v + v_t)\left(\frac{\partial u_i}{\partial x_j} + \frac{\partial u_j}{\partial x_i}\right)\right)$$

Energy equation

$$\frac{\partial u_i T}{\partial x_i} = \rho\frac{\partial}{\partial x_i}\left(\left(\frac{v}{Pr} + \frac{v_t}{Pr_t}\right)\frac{\partial T}{\partial x_i}\right)$$

Where u_i T, and Pr represent the fluid velocity, temperature and pressure, respectively. ρ is the fluid density, v and Pr are the fluid kinematic viscosity and Prandtl number, subscript t refers to turbulent flow.

Realizable $k-(\varepsilon)$ epsilon turbulence model is adopted in the current study because it can provide superior performance for flows involving boundary layers effect under strong adverse gradient of pressure.

Turbulent kinetic energy ***k*** equation:

$$\frac{\partial u_i k}{\partial x_i} = \frac{\partial}{\partial x_i}\left(\left(v + \frac{v_t}{\sigma_x}\right)\frac{\partial k}{\partial x_i}\right) r - \varepsilon$$

Turbulent energy dissipation ε equation

$$\frac{\partial u_i \varepsilon}{\partial x_i} = \frac{\partial}{\partial x_i}\left(\left(v + \frac{v_t}{\sigma_\varepsilon}\right)\frac{\partial \varepsilon}{\partial x_i}\right) + c_1 r \varepsilon - c_2 \frac{\varepsilon^2}{k + \sqrt{v\varepsilon}}$$

Where r represents the generation of turbulence kinetic energy, *k* due to the mean velocity gradients and is given by:

$$r = -\overline{u_i u_j}\frac{\partial u_i}{\partial x_i} = v_{turb}\left(\frac{\partial u_i}{\partial x_j} + \frac{\partial u_j}{\partial x_i}\right)\frac{\partial u_i}{\partial x_j}$$

The turbulent kinematic viscosity is:

$$v_t = c_\mu \frac{k^2}{\varepsilon},$$

One of the most important parts of simulation process is selecting a suitable meshing process to calculate fundamental equations governing the heat-exchanger operation. The soft wares Gambit and Fluent were used to mesh the models and to simulate the system, respectively. Selecting a proper meshing can contribute to a suitable convergence in solving the equations while an improper meshing can lead to instability and divergence of calculations. Figure 2 reveals some parts of the geometry used to simulate the system. The grid design implemented

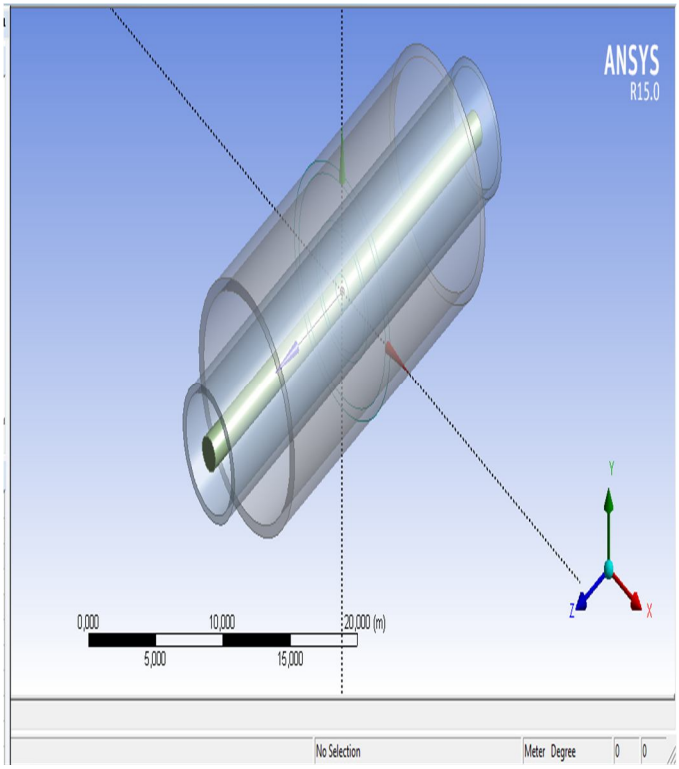

Fig.2. Double pipe heat exchanger with circular strip.

By the authors in this work is an improvement of those structures proposed by previous researchers. There were a number of assumptions, some of which are presented in the following lines, which simplified the simulation in the present study. The fluid utilized in this work was the water (a Newtonian fluid), and its properties were estimated depending upon the temperature of the media when it flowed along the tube inside the heat-exchanger. The properties of the oil utilized in both the experiments and simulation process are shown in Table 1. The fluid thermo physical properties varied piecewise-linear with fluid temperature At steady condition, the fluid flow was considered to be turbulent at Reynolds numbers of 100-1200 [19] No slip condition was considered for the system wall. The fully developed turbulent profile in a pipe at a constant rate and temperature of 303 K, associated with a uniform static pressure, was applied to the tube's inlet. In addition to considering no thickness for tube walls, a constant temperature 313 K was simply set throughout the heat-exchangers. Except gravity force, other body forces and viscous dissipation were neglected. To calculate LMTD, only the surface average temperature of the fluid at both sides of heat-exchangers was used. Since the fluid entered the heat-exchanger has passed a long distance before its entrance, it was necessary to impose the fully developed velocity profile condition at the inlet of the heat-exchanger. It is needless to say that to adapt the inlet boundary condition according to its experimental circumstances, the Fluent users have to introduce a user defined- function (CFD) program

and import it into the Fluent program. This part shows the effect of the circular strip inserts as well as the Reynolds number on the Nusselt number and friction factor. Before that, to study the grid independence in the heat exchanger, several mesh structures with different mesh densities for the 3D heat-exchanger were generated. The results of the simulations for the double pipe heat exchanger with the longitudinally circular strip. The region near to the strip was meshed finer than the rest of the section in order to compute the values of variables with high gradients near the walls.

To obtain the temperature and velocity field inside the heat exchangers, Semi- Implicit Pressure Linked Equations (SIMPLE) scheme which is a branch of the pressure velocity coupling method was used for the simulations. The second order upwind discretization scheme for momentum and energy was employed in order to determine the variables inside each cell. As the Green-Gauss Node-Based is the most accurate method with respect to others, it was chosen for the present work to find the variables' gradient. Simulations were carried out until the value of residual for continuity and temperature variables reached and, respectively. The computer used for this study was a core i7 processor with 40 GHz CPU and 16 GB RAM-memory. Regarding the residual criteria, the average time required for each run was about 12 hrs. The results and discussion taken from several runs are presented in the proceedings.

III. RESULTS AND DISCUSSION

The computed results are used to calculate the heat transfer coefficients for different configurations from the numerical temperature field by using Newton's cooling law. As specified in the boundary conditions in FLUENT, outlets on both sides are assumed to have a zero pressure; thus, the pressure drop in both annulus and inner tube side is equal to the inlet pressure for each side. It is noted that the simulations are based on the assumption that the initials conditions for different mass flow rate and different shapes, i.e., the inlet temperatures and mass flow rates of the working fluids, are identical.

A. Model Validation

A numerical model was used to evaluate the heat transfer and pressure drop characteristics of a double pipe heat exchanger with longitudinal strip (circular and square). This numerical model was validated by comparing its results with experimental data for a double-pipe heat exchanger with longitudinal strip as obtained using empirical correlations under turbulent flow conditions.

B. Heat transfer Performance of a Heat Exchanger with Longitudinal Circular Strip

The pressure drop and the heat transfer rate are used to characterize the heat exchanger performance. These parameters determine the pumping power and size requirements of the heat exchanger.

Both pressure drop and thermal performance are affected by a number of parameters such as the geometry of the heat exchanger and flow conditions. The numerically analysis is calibrated with experimental test section, water as working fluid. The hot water is flowing through the inside tube and cold water is flowing through the annulus tube.

The rate of heat flow through the tube side is calculated from Eq. (2) and the rate of heat flow through the annulus is calculated from Eq. (3) and observed that the difference is ±2.5%. The annulus side heat transfer coefficient h_o is calculated from Eq. (10) and the tube side heat transfer coefficient h_i is calculated from Eq. (11) this h_i and h_o values are substituted in Eq. (5) for the calculation of tube side overall heat transfer coefficient u_i.

The experimental Nusselt number is calculated using the Eq. (11) based on the tube side heat transfer coefficient, thermal conductivity of the hot water and diameter of the tube. The deviation between the experimental values and theoretical values presents a maximum value of ±2.5%, which means the heat loss from the experimental test section is practically negligible.

The temperature drop in the tube side is neglected because the inner tube is a smooth tube and outer surface of the tube is insulated and the mass flow rates of the working fluid are very high.

Therefore, the experimental setup is well designed and it is gives further confidence about the reliability of results obtained with different mass flow rates of the hot fluids. The viscosity value at bulk mean temperature of hot fluid is used for the estimation of Reynolds number is calculated using the Eq. (12), it is used for the estimation of inside heat transfer coefficient of different mass flow rates are calculated based on the heat transfer coefficient, thermal conductivity value at bulk mean temperature and the diameter of the test tube.

The Fig. 4 represents the Nusselt number values of different mass flow rates of hot fluid and different sizes of longitudinally circular strips are placed inside of the tube. It is observed that Nusselt number of hot fluid is increases with increase mass flow rate and Reynolds numbers and size of the circular strip.

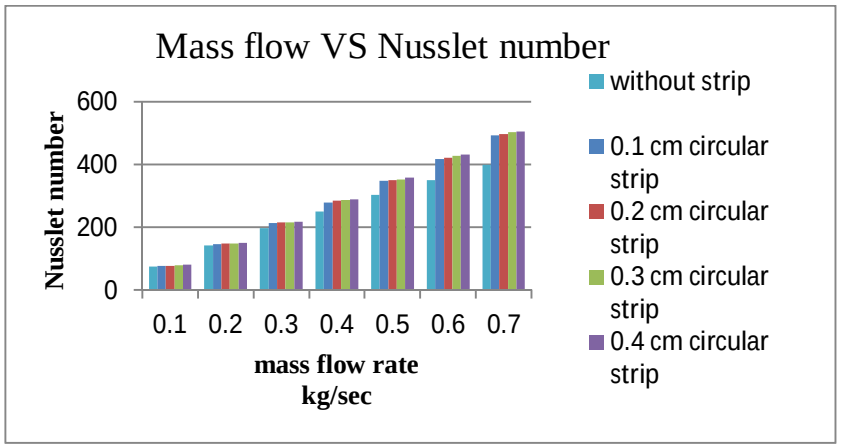

Fig.4. Comparison of the Nusselt number of tube side hot water with different mass flow rate.

The mass flow rate of hot fluid is increased from 0.1 to 0.7 kg/sec, and then the nusslet number is also increased from 77 to 550 nearly.

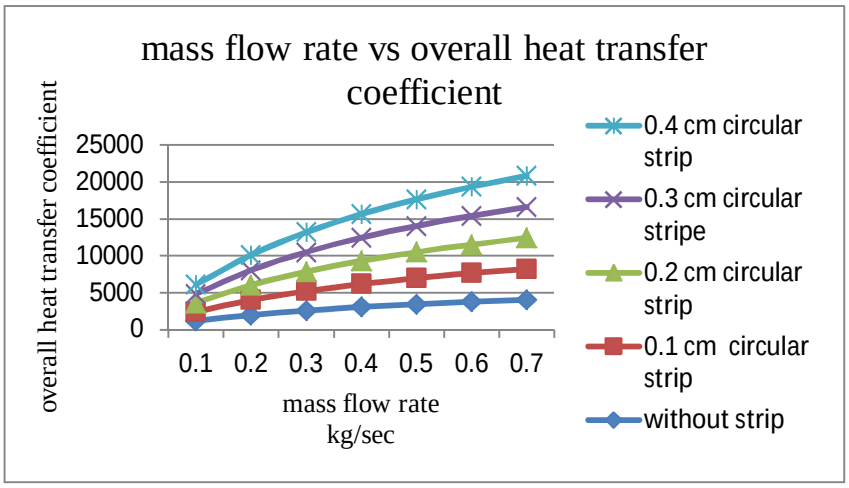

Fig.5. Comparison of the overall heat transfer coefficient of tube side hot water with different mass flow rate.

The Fig. 5 represents the overall heat transfer coefficients at different mass flow rates of hot fluid and different sizes of longitudinal circular strips. It is observed that the overall heat transfer coefficient of hot fluid increases with increase of mass flow rate, Reynolds numbers and size of the circular strip.

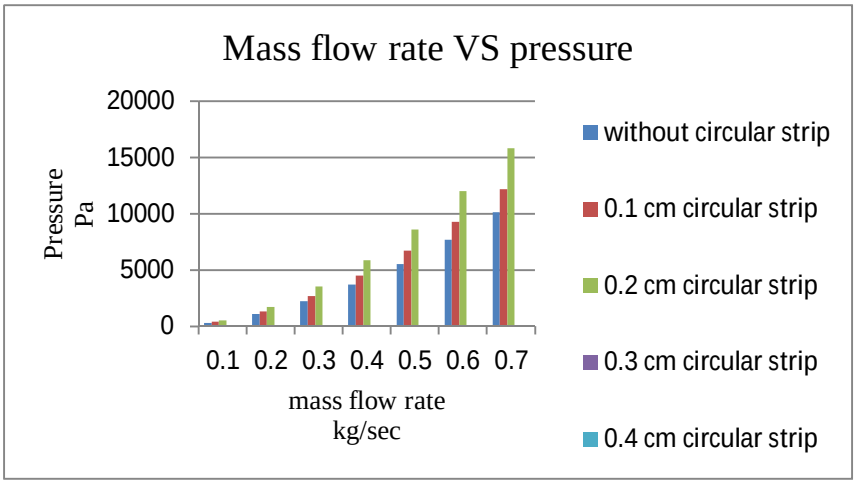

Fig.6. Comparison of the pressure of tube side hot water with different mass flow rates.

The Fig. 6 represents the pressure drop at different mass flow rates of hot fluid and different sizes of longitudinal circular strips. It is observed that the pressure drop of hot fluid increases with increase of mass flow rate, Reynolds numbers and size of the circular strip.

C. Heat transfer Performance in Square Strip

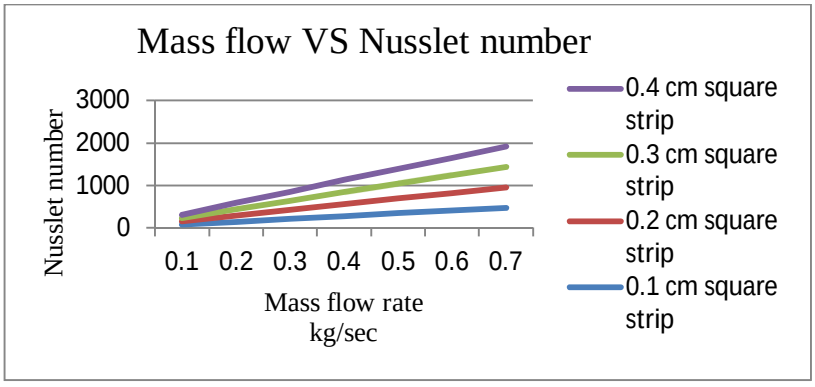

Fig.7. Comparison of the Nusselt number of tube side hot water with different mass flow rate.

The Fig.7 represents the Nusselt number values at different mass flow rates of hot fluid and different sizes of longitudinal square strips are placed inside of the tube. It is observed that Nusselt number of hot fluid increases with increase mass flow rate and Reynolds numbers and size of the square strip.

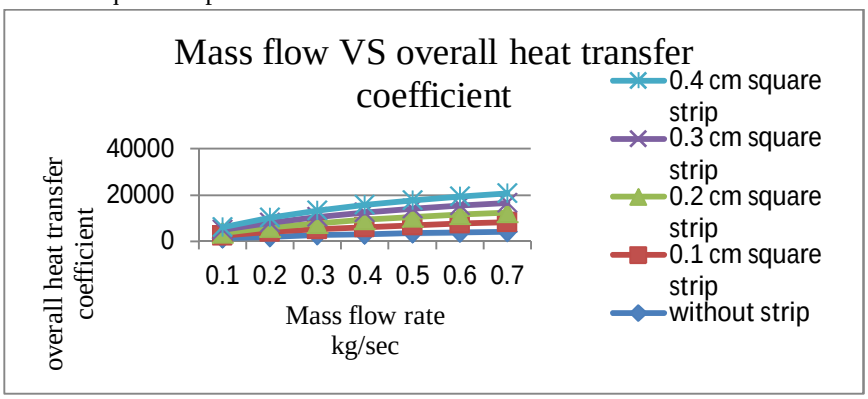

Fig.8. Comparison of the overall heat transfer coefficient of tube side hot water with different mass flow rate.

The Fig. 8 represents the overall heat transfer coefficients at different mass flow rates of hot fluid with different sizes of longitudinal square strips. It is observed that the overall heat transfer coefficient of hot fluid increases with increase of mass flow rate, Reynolds numbers and size of the square strip.

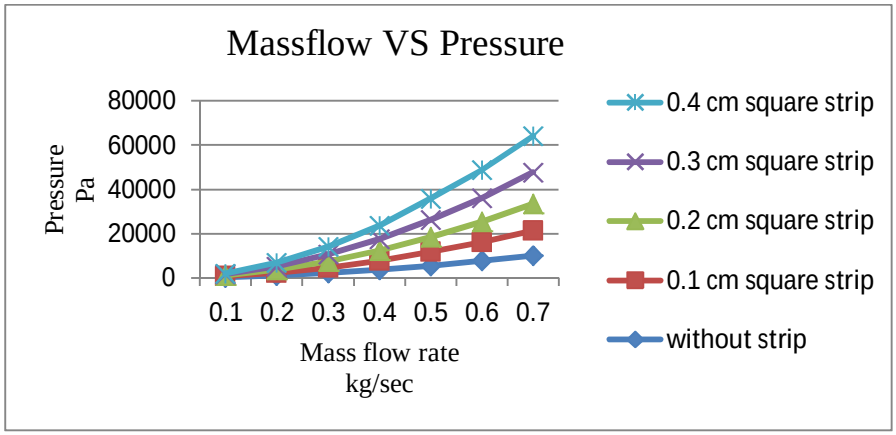

Fig.9. Comparison of the pressure of tube side hot water with different mass flow rates.

The Fig. 9 represents the pressure drop at different mass flow rates of hot fluid with different sizes of longitudinal square strips. It is observed that the pressure drop of hot fluid increases with increase of mass flow rate and Reynolds numbers and size of the square strip.

D. Comparisons between THe Circular And Square Strips

Comparisons are drawn between the circular strips of different sizes which are inserted inside the heat exchangers and also compared with the heat exchangers without any insertion of strip. After analysing at different mass flow rates it is observed that heat transfer rate is more with the insertion of circular strip and less when compared to normal heat ecxhnager. It is also clear that, as the size of the circular strip increases heat transfer rate increases and is also observed that it is more when compared with the square strip.

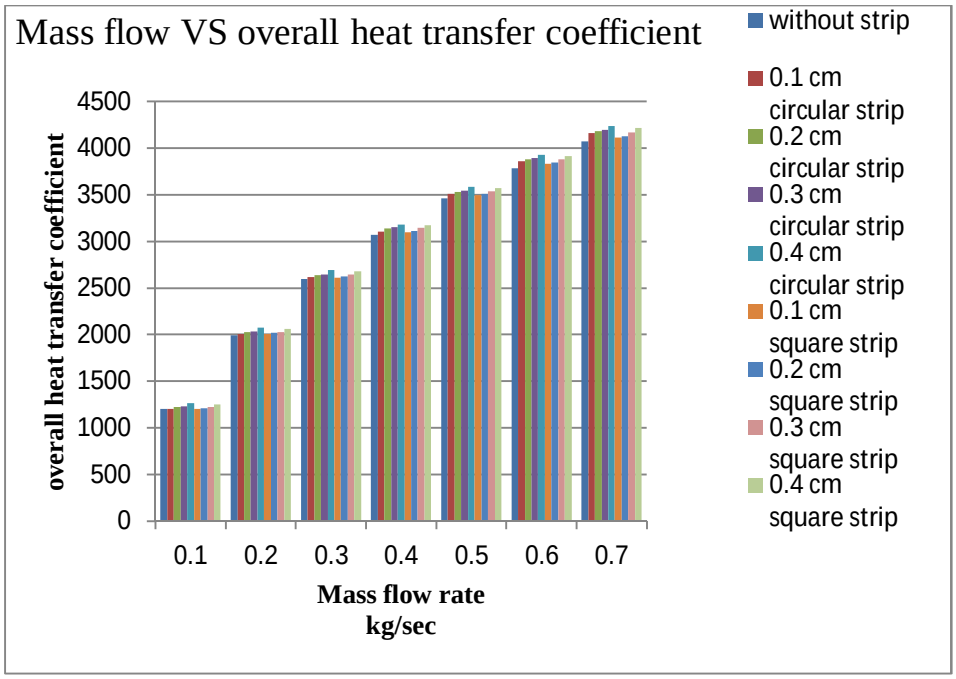

Fig.10. Comparison of the overall heat transfer coefficient of tube side hot water with different mass flow rates and the different geometries.

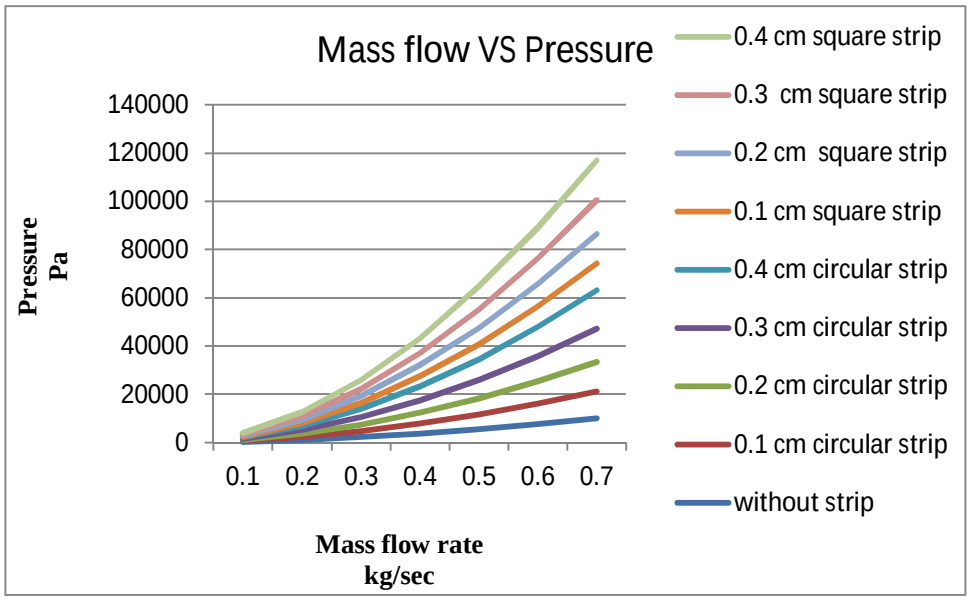

Fig.11. Comparison of the pressure of tube side hot water with different mass flow rates and the different geometries.

The heat transfer performance of double pipe heat exchanger with and without longitudinal strip is placed inside the tube. The different shapes of the strips are used in this analysis as the circular strip and square strips with different mass flow rates. In this numerical analysis is done on circular and square strips which are placed inside the inner tube of double pipe heat exchanger. It is observed that the pressure drop in the heat exchanger with strip is higher than the without strip of the double pipe heat exchanger with different mass flow rates. The graph of double pipe heat exchanger is shown here by comparing circular with square strip. The pressure drop in the double pipe heat exchanger with square strip is higher than the circular strip with different mass flow rates.

IV. CONCLUSIONS

The present work focuses on the estimation of heat transfer, pressure drop and overall heat transfer coefficient of different mass flow rates in a double pipe heat exchanger with and without different geometries strip. The heat transfer of hot fluid increases with increasing mass flow rate and Reynolds number. There is further enhancement with insertion of the square and circular stripes with different sizes. The pressure drop is increased with increased mass flow rate and size of the stripes.

V. ACKNOWLEDGMENT

I would like to manifest my heartier thankfulness pertaining to my contentment to Mrs. G. Srivalli, Assistant professor for guiding me with adroit commitment and excellence. This has helped in bringing out this project work with artistry. We are extremely indebted for this kind help. We are perspicuous to divulge our sincere gratefulness to Dr. N.VIJAYA SAI, Head of the Department, Department of Mechanical Engineering for his constant encouragement and assistance to us, which contribute to the successful completion of this project. I express my sincere thanks to the college management for providing all the lab and library facilities required for completing my project successfully.

REFERENCES

[1] N.T. Ravi Kumar, L. Syam Sundar, P. Bhramara, Manoj K. Singh, Antonio C.M. Sousa, “Heat transfer, friction factor and effectiveness of Fe3O4 nanofluid flow in an inner tube of double pipe U-bend heat exchanger with and without longitudinal strip inserts” International Journal of Heat and Mass Transfer 109 (2017) 440–453.
[2] L. Syam Sundar, P. Bhramara, N.T. Ravi Kumar, Manoj K. Singh, Antonio C.M. Sousa, “Experimental heat transfer, friction factor and effectiveness analysis of Fe3O4 Nano fluid flow in a horizontal plain tube with return bend and wire coil inserts” Experimental Thermal and Fluid Science 85 (2017) 331–343
[3] Manoj K. Singh, L. Syam Sundar, P. Bhramara, N.T. Ravi Kumar , Antonio C.M. Sousa, “Heat transfer, friction factor and effectiveness analysis of Fe3O4/water Nano fluid flow in a double pipe heat exchanger with return bend” International Communications in Heat and Mass Transfer 81 (2017) 155–163
[4] Hiroyuki Shiraiwa, Yutaku Kita, “Performance improvement of a falling-film-type heat exchanger by insertion of shafts with screw blade in a heat exchanger tube” Applied Thermal Engineering 102 (2016) 55–62
[5] Rafal Andrzejczyk, Tomasz Muszynski, “Thermodynamic and geometrical characteristics of mixed convection heat transfer in the shell and coil tube heat exchanger with baffles” Applthermaleng.2017.04.053
[6] Yonggang Leia , Yazi Lia , Shenglan Jinga , Chongfang Songa , Yongkang Lyub , Fei Wang , “Design and performance analysis of the novel shell-and-tube heat exchangers with louver” Applthermaleng.2017.07.081.
[7] Piotr Wais, “Correlation and numerical study of heat transfer for single row cross-flow heat exchangers with different fin thickness” Procedia Engineering 157 (2016) 177 – 184.
[8] Daniele Fiaschi a, Giampaolo Manfrida , Luigi Russo, Lorenzo Talluri , “Improvement of waste heat recuperation on an industrial textile dryer: Redesign of heat exchangers network and components” Energy Conversion and Management (2017).
[9] Gholamreza Bamorovat Abadi1, Kyung Chun Kim, “Experimental Heat Transfer and Pressure Drop in a Metal-Foam-Filled Tube Heat Exchanger,” expthermflusci.2016.10.031.
[10] Kashif Nawaz a, Jessica Bock b , Anthony M. Jacobi, “Thermal-hydraulic performance of metal foam heat exchangers under dry operating conditions”, Applied Thermal Engineering 119 (2017) 222–232.
[11] Javier Bonillaa,b, Alberto de la Callec , Margarita M. Rodr´ıguez-Garc´ıaa , Lidia Rocaa,b, Loreto Valenzuela, “Study on Shell-and-Tube Heat Exchanger Models with Different Degree of Complexity for Process Simulation and Control Design” applthermaleng.2017.06.129
[12] QIAN Jin1, KONG Qiao-Ling, ZHANG Hong-Wu , ZHU Zhi-Hong, HUANG Wei-Guang, Li Wen-Hui, “Experimental Study for Shell-and-Tube Molten Salt Heat Exchangers” applthermaleng.2017.06.005.
[13] Bao-Cun Du, Ya-Ling He, Kun Wang, Han-Hui Zhu, “Convective heat transfer of molten salt in the shell-and-tube heat exchanger with segmental baffles” International Journal of Heat and Mass Transfer 113 (2017) 456–465.
[14] Mehmet Tana, Rasim Karabacak, Mustafa Acar, “Experimental assessment the liquid/solid fluidized bed heat exchanger of thermal performance” Geothermics 62 (2016) 70-78
[15] Wang a ,Zhen Tian a ,Bo Gu , Bing Wu ,Hongtao Ma ,Cheng Qian , “Experimental study on the liquid-side characteristics of meso-channel heat exchangers in fuel cell vehicles” Applied Thermal Engineering 96 (2016) 258–266.

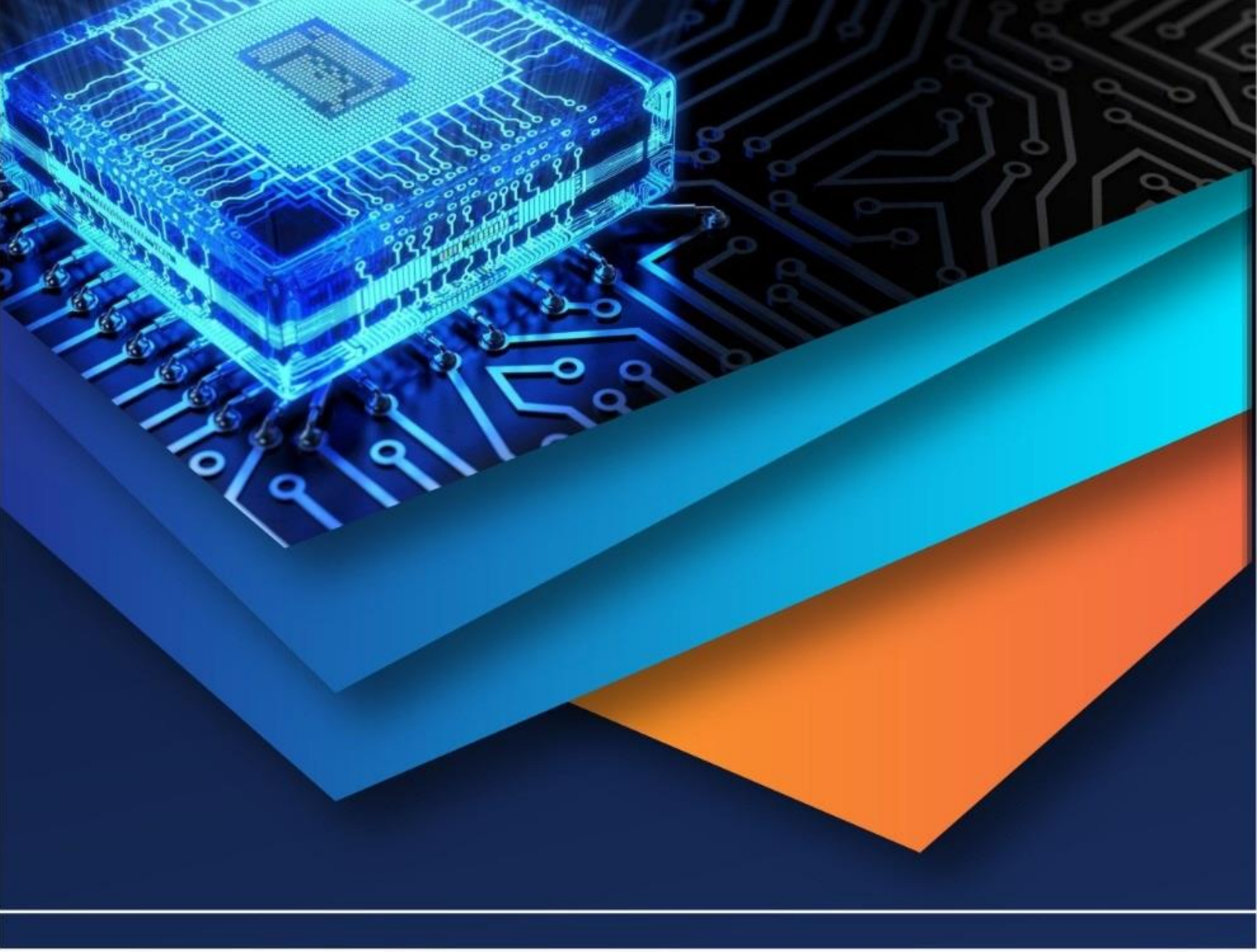

10.22214/IJRASET

45.98

IMPACT FACTOR: 7.129

IMPACT FACTOR: 7.429

INTERNATIONAL JOURNAL FOR RESEARCH

IN APPLIED SCIENCE & ENGINEERING TECHNOLOGY